Plasmonic Nanosensors for Simultaneous Quantification of Multiple Protein–Protein Binding Affinities

ARTICLE *in* NANO LETTERS · AUGUST 2014

Impact Factor: 13.59 · DOI: 10.1021/nl501865p · Source: PubMed

8 AUTHORS, INCLUDING:

Janak Prasad
Centre d'Élaboration de Matériaux et d'Etudes…
6 PUBLICATIONS **147** CITATIONS
SEE PROFILE

Andreas Henkel
Johannes Gutenberg-Universität Mainz
13 PUBLICATIONS **299** CITATIONS
SEE PROFILE

Dirk Schneider
Johannes Gutenberg-Universität Mainz
87 PUBLICATIONS **1,580** CITATIONS
SEE PROFILE

Germán Rivas
Spanish National Research Council
101 PUBLICATIONS **2,680** CITATIONS
SEE PROFILE

NANO LETTERS

Letter

pubs.acs.org/NanoLett

Plasmonic Nanosensors for Simultaneous Quantification of Multiple Protein–Protein Binding Affinities

Rubén Ahijado-Guzmán,[†] Janak Prasad,[†,‡] Christina Rosman,[†] Andreas Henkel,[†] Lydia Tome,[§] Dirk Schneider,[§] Germán Rivas,*[,∥] and Carsten Sönnichsen*[,†]

[†]Institute of Physical Chemistry, University of Mainz, Duesbergweg 10-14, D-55128 Mainz, Germany

[‡]Graduate School Materials Science in Mainz, University of Mainz, Staudingerweg 9, D-55128 Mainz, Germany

[§]Institute of Pharmacy and Biochemistry, University of Mainz, Johann-Joachim-Becher-Weg 30, D-55128 Mainz, Germany

[∥]Centro de Investigaciones Biológicas, CSIC, c/Ramiro de Maeztu 9, 28040 Madrid, Spain

S *Supporting Information*

ABSTRACT: Most of current techniques used for the quantification of protein–protein interactions require the analysis of one pair of binding partners at a time. Herein we present a label-free, simple, fast, and cost-effective route to characterize binding affinities between multiple macromolecular partners simultaneously, using optical dark-field spectroscopy and individual protein-functionalized gold nanorods as sensing elements. Our NanoSPR method could easily become a simple and standard tool in biological, biochemical, and medical laboratories.

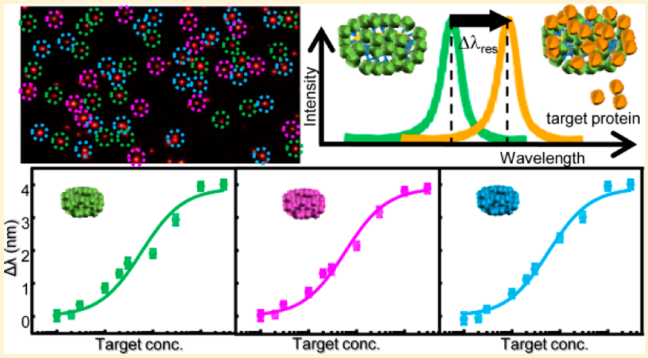

KEYWORDS: *NanoSPR, plasmonic nanosensors, multiple protein–protein interactions, optical dark-field spectroscopy, FtsZ*

The dynamics in living organisms is governed by a complex network of interacting macromolecules.[1−3] For example, in a process like cell division a dozen of proteins interacts in a subtle and interconnected way of subprocesses to finally define a division place or to generate the constriction force in the cell wall.[4−6] To fully understand, model, and potentially influence such a process, it is important to quantify binding affinities between all possible partners, preferentially without introducing fluorescent labels. Popular techniques to do so are surface plasmon resonance (SPR) biosensors,[7] quartz crystal microbalance,[8] fluorescence correlation spectroscopy,[9] isothermal titration calorimetry,[10] or analytical ultracentrifugation.[11] However, most of the label-free techniques used to study binding affinities require the analysis of one pair of binding partners at a time, making the quantification of a complex interaction network a laborious and slow effort. While there are some approaches described to increase the throughput by effectively building several experiments into one device, for example, electro-switchable sensors,[12] multiflow-channel SPR chips,[13] or microring resonators,[14] these approaches are expensive compared with nanoparticles and not as easily upscalable.

We have tackled this problem in a novel way by employing individual gold nanorods as sensing elements. Each gold nanorod responds to binding events near its surface by a shift in the plasmon resonance wavelength.[15−17] The nanorods are connected to proteins via specific tags, making it simple to generate a library of nanoparticles, each functionalized with a different type of protein P_1 ... P_i. Particles from this library are deposited on a common substrate for simultaneous quantification of the interaction of proteins P_1 ... P_i with a common target molecule T. We demonstrate the power of this easily upscalable approach by determining the binding affinities of three essential cell division proteins to the target FtsZ, a protein involved in constriction of the cell envelope during prokaryotic cell division.[4,5]

Our "NanoSPR" method provides a simple, fast, and cost-effective route to characterize binding affinities between many macromolecular partners simultaneously. This technique could become a simple standard tool in biological, biochemical, and medical laboratories, where protein interactions with multiple partners are studied, for example, in drug discovery projects, when active substances are screened for potential interference with cellular processes.

The main challenge to develop plasmonic nanosensors as a general tool for the characterization of macromolecular binding affinities is to develop a general functionalization strategy to connect the nanoparticles with a given protein P_i. In protein biochemistry, (reversible) protein adsorption via so-called "His-tags" is well-established, where histidine residues (His) complex

Received: May 20, 2014
Revised: August 4, 2014
Published: August 25, 2014

   dx.doi.org/10.1021/nl501865p | *Nano Lett.* 2014, 14, 5528−5532

a metal ion (e.g., Ni^{2+}) bound to a nitrilotriacetic acid (NTA) group. Because this method is often used in protein purification, numerous physiologically relevant proteins are already available with genetically fused His-tags. It is well established that the reversible Ni^{2+}-His interaction (in most cases) does not interfere with protein function. Therefore, we developed a strategy for the functionalization of gold nanorods with NTA while keeping the nanoparticles stable in solution (Figure 1a). A stable stock of Ni^{2+}- NTA-functionalized gold

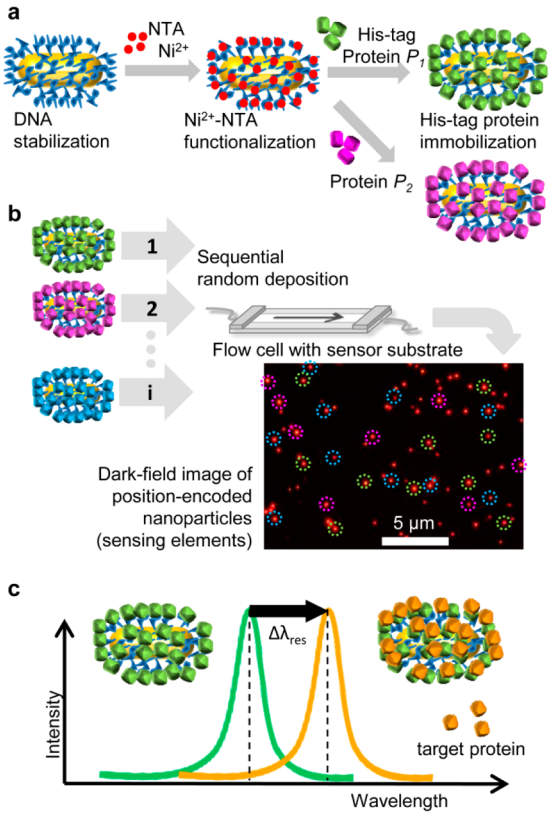

Figure 1. Principle of NanoSPR: particle functionalization, sensor fabrication, and detection principle. (a) Scheme of the two-step functionalization strategy used to immobilize a protein P_i on gold nanoparticles. (b) Consecutive deposition of particles 1...*i* while recording their positions after each deposition step creates a position encoded sensor (inset). The inset shows a dark-field image of the resulting randomly deposited gold nanorods. Each nanorod serves as a sensing element for a specific protein−target interaction. (c) The binding of target proteins *T* injected into the flow cell to nanoparticles covered by proteins P_i produces a shift $\Delta\lambda_{res}$ in the plasmon resonance.

nanorods (AuNRs@Ni^{2+}-NTA) provides an easy way to create a library of His-tagged protein-functionalized nanorods by simply adding proteins P_i to small aliquots of the (AuNRs@ Ni^{2+}-NTA) stock solution.

However, the NTA functionalization must provide sufficient colloidal stability in buffers commonly used in a biological settings.[18] From synthesis, gold nanorods are typically stabilized with the surfactant cetyltrimethylammonium bromide (CTAB), which does, however, not prevent particle aggregation in saline buffers at physiological ionic strength. Direct substitution of CTAB by NTA does not yield sufficiently stable particles as well. Therefore, we stabilize the gold nanorods first with short bifunctional DNA strands, consisting of 11 thymidine bases and a thiol/amine group at their ends. The thiol group readily binds to gold whereas the amine group is used to specifically couple with isothiocyanobenzyl-NTA in buffered aqueous solution. Established methods for the conjugation of gold nanorods with proteins employ either surfactants,[19] polyelectrolytes,[20] or small thiolated molecules. In the first two cases, a surfactant (Brij 56) or polyelectrolyte (PSS) is first adsorbed onto the CTAB layer. In the third method, the CTAB layer on the gold nanorod is exchanged with small ligand molecules, such as cystamine,[21] mercaptoundecanoic acid,[22] or thiolated polyethylene glycols.[23] Additionally, thiolated proteins can directly bind to the gold nanorod surface via ligand exchange.[23] The drawback of all the above methods is that a random site on the protein is conjugated to the gold surface, which could lead to some loss of the protein function. Moreover, direct attachment of proteins via ligand exchange could even lead to protein denaturation on the gold surface.

To proof the concept of our novel multiplexed NanoSPR method, we deposit four batches of gold nanorods on our sensor substrate, three functionalized with different proteins P_1, P_2, P_3 and one nonfunctionalized as reference. By flowing in one batch at a time while recording the position of each randomly deposited nanoparticle, we know the specific functionalization for each particle on the sensor surface, thus effectively generating a position-encoded sensor, similar to a spotted array but without any geometrical order (Figure 1b).[24] It should be noted that all particles look exactly the same (on average) and only the (recorded) position on the substrate allows us to assign them a specific functionality.

The binding of a common target protein *T* to the previously deposited functionalized gold nanorods causes a shift in the plasmon wavelength $\Delta\lambda_{res}$ as schematically shown in Figure 1c. The plasmon shift of each single gold nanoparticle sensor is recorded by optical dark-field spectroscopy for every particle in the field of view, using a fully automated, temperature stable, user-friendly, and fast optical microscopy system optimized for spectral precision. This system allows the routine recording of the response of hundreds of particles with a precision of about 0.3 nm.[24] Using the assignment of every particle to one of the functional groups (Figure 1b), we can assign the measured responses to the different interaction pairs.

We demonstrate our NanoSPR concept by studying the interaction of three bacterial division proteins (MinC and two soluble variants of ZipA, s1- and s2-ZipA, lacking its transmembrane domain, see Supporting Information) with its target protein, FtsZ (a 40 kDa soluble GTPase, homologue of eukaryotic tubulin[4,5]), an essential element of the division machinery of most bacterial systems. In *Eschericia coli*, FtsZ is anchored to the cytoplasmic membrane by the action of the membrane protein ZipA (a 36.4 kDa trans-membrane protein, containing the FtsZ binding-domain at the globular cytoplasmic C-terminal region[25]) and the amphitropic protein FtsA. Together they form the initial assembly of the division machinery (the proto-ring complex), which drives cytokinesis at midcell, where FtsZ polymers form a dynamic Z-ring active in division.[26] The MinCDE system is one of the two control mechanisms that cooperates in the correct positioning of the division ring by inhibiting ring formation in wrong places. MinC is a 24 kDa protein that prevents FtsZ assembly.[27,28]

To evaluate the binding affinities of these three interacting pairs (FtsZ-s1ZipA, FtsZ-s2ZipA, and FtsZ-MinC), the sensor was exposed to solutions with increasing FtsZ concentrations, similar to the titration method described by Schuck.[29] FtsZ aliquots were flowed into the flow cell until the interaction with

dx.doi.org/10.1021/nl501865p | *Nano Lett.* 2014, 14, 5528−5532

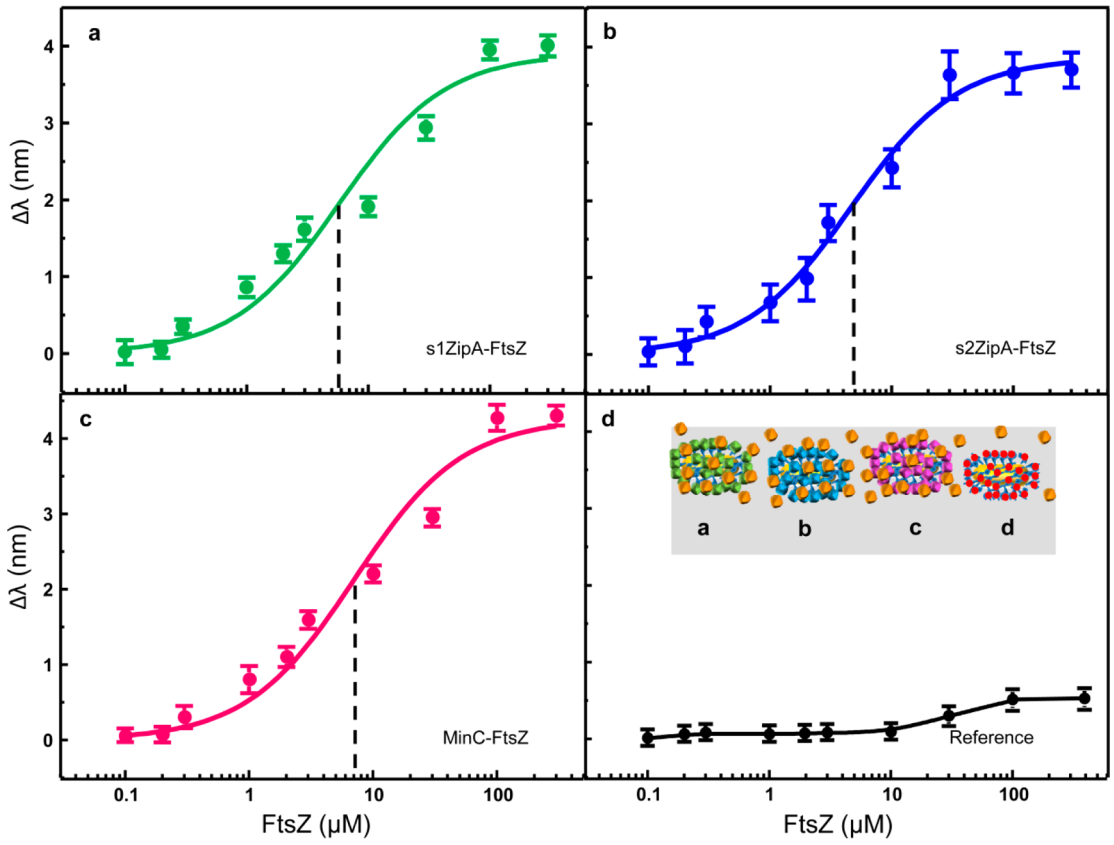

Figure 2. Binding affinity of multiple protein−protein interactions. The data points in the four subpanels correspond to the mean plasmon shift $\Delta\lambda_{res}$ measured on 20−50 nanoparticles covered by (a) s1-ZipA, (b) s2-ZipA, (c) MinC, and (d) no protein. The error bar indicates the standard error of the mean. The plasmon shifts $\Delta\lambda_{res}$ are measured for increasing concentrations of the target protein FtsZ (after equilibration) and obtained on a single NanoSPR sensor. The solid lines correspond to the best fit of a Langmuir equation to the experimental data, used to extract the K_D values listed in Table 1 (dashed lines).

Table 1. log K_D Values Obtained in Present Work by NanoSPR and SPR Together with Literature Values Determined by Composition Gradient-Static Light Scattering (CG-SLS), Sedimentation Equilibrium-Analytical Ultracentrifugation (SE-AUC), and Fluorescence Anisotropy (FA)

	NanoSPR	SPR	GC-SLS	SE-AUC	FA
FtsZ-s1ZipA	5.2 ± 0.2	5.4 ± 0.1	5.8 ± 0.1[32]	5.4[32]	
FtsZ-s2ZipA	5.3 ± 0.1	5.3 ± 0.2			
FtsZ-MinC	5.1 ± 0.1	5.0 ± 0.1			4.9 ± 0.1[30]
FtsZ-ZipA wt				6.1 ± 0.5[31]	

the sensors reached equilibrium.[7] After about 20 min, we recorded the wavelength shift $\Delta\lambda_{res}$ of about 200 particles, which gave about 30−50 data points for each interaction pair. Figure 2 shows the average plasmon shift $\Delta\lambda$ as a function of FtsZ concentration, that is, the binding isotherms, for each of the three interacting pairs and the nonfunctionalized reference particles. The flat response of the reference particles demonstrated that unspecific interactions between the sensors and FtsZ are negligible. The experimental data are well described by the Langmuir equation $\Delta\lambda/\Delta\lambda_{max} = cK_D/(1 + cK_D)$, which allows us to extract the equilibrium dissociation constants K_D for each pair. The values for the three interacting pairs are listed in Table 1 and are in excellent agreement with values previously obtained by composition-gradient static light scattering (CG-SLS), sedimentation equilibrium-analytical ultracentrifugation (SE-AUC), fluorescence anisotropy (FA)[30−32] or in independent titration measurements performed with the conventional SPR (Supporting Information, Figure S4). In contrast to all other techniques, our NanoSPR results were obtained simultaneously on a single sensor, providing binding affinities for all three proteins and the reference.

Regeneration and reusability are important aspects of sensors. It is well-known that NTA-Ni^{2+}-His-tag complexes are easily broken up by adding an excess of the Ni^{2+}-complexing imidazole. To demonstrate that this also works in case of the NanoSPR we tested the removal of s1ZipA from Ni^{2+}-NTA functionalized gold nanorods by washing with imidazole. Addition of s1ZipA to the nanorods leads to the expected plasmon shift $\Delta\lambda$, which fully reversed to its original position after washing with imidazole (Figure 3a). Repeating this cycle three times showed very little degeneration of the sensor. However, we should mention that a multiplexed sensor, containing groups of particles functionalized with different proteins, cannot be recycled in this way because subsequent protein addition will affect all particles simultaneously. More sophisticated orthogonal binding chemistry or microfluidic

dx.doi.org/10.1021/nl501865p | Nano Lett. 2014, 14, 5528−5532

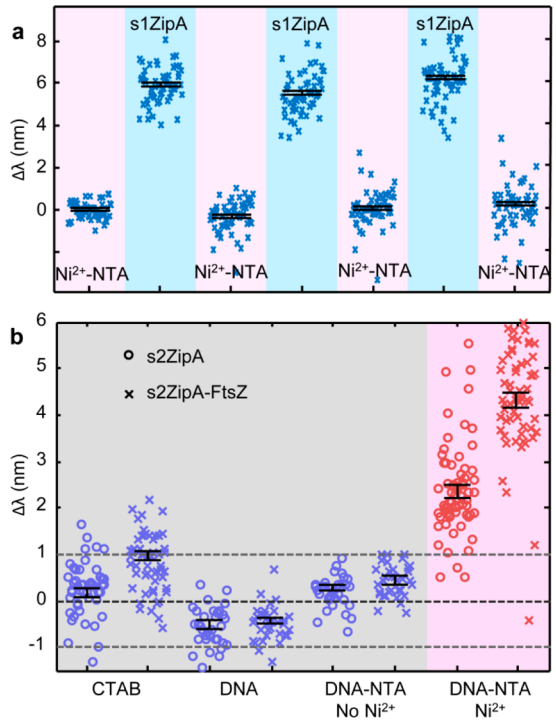

Figure 3. Control experiments. (a) Sensor response after repeated incubation with s1ZipA (1 μM, light-blue-shaded areas) and imidazole (800 mM, pink-shaded areas). The actual measurements were conducted in both cases in the same working buffer. Each small cross represents the response of an individual nanoparticle and the black symbols represent the median and its standard error for all 47 particles. The plasmon shift $\Delta\lambda_{res}$ reversed to its original value after each cycle. (b) To demonstrate the power of the two-step functionalization strategy, we exposed four kinds of particles to the proteins. These particles where covered with (1) CTAB, (2) DNA, (3) DNA+NTA, or (4) DNA+NTA+Ni^{2+}. Upon addition of the His-tagged protein s2ZipA (0.5 μM), the last group showed the expected large plasmon shift, indicative of an efficient protein immobilization. (The mean shift is smaller than that observed in panel (a) because of the smaller molecular mass of s2ZipA (16.4 kDa) compared to s1ZipA (34.2 kDa)). The CTAB particles showed some smaller nonspecific affinity, whereas the DNA coating completely prevents unspecific protein binding. The fact that the addition of FtsZ (2 μM) leads to an additional shift proves that s2ZipA maintains its FtsZ binding affinity after immobilization on the nanoparticle surface.

control of protein placement would be necessary to recycle multiplexed sensors. However, the fast and simple fabrication process of our sensors by random deposition does, in our opinion, not make this effort worthwhile.

To demonstrate the effectiveness of our two-step protein functionalization procedure, we expose four types of gold nanorods first to a protein with a His-tag (s2ZipA) and then to FtsZ: gold nanorods directly from synthesis (presumably with a CTAB layer), nanorods stabilized with DNA, and DNA-NTA functionalized nanorods in the absence and presence of Ni^{2+} ions. Only the NTA functionalized nanorods in the presence of Ni^{2+} ions show large plasmon shifts after adding s2ZipA (Figure 3b), indicating the successful immobilization of s2ZipA via the His-tag. The gold nanorods used directly from synthesis show a small plasmon shift, presumably from unspecific adsorption of s2ZipA to the (more or less) unprotected gold surface. The DNA stabilization seems to protect the nanoparticles from this unspecific adsorption, as evident from the small plasmon shifts. The fact that further addition of FtsZ leads to an additional plasmon shift only in the case of DNA-NTA-functionalized gold nanorods in the presence of Ni^{2+} ions demonstrates that the immobilized s2ZipA maintains its FtsZ binding function.

The data presented in Figure 3 also demonstrates another point: the spread of the plasmon shifts observed between different nanoparticles is larger in some cases than in others although all experiments are performed from the same batch of gold nanorods. Only differences in the number of receptor and/or target molecules bound to a specific nanoparticle can explain this.

Taking the results presented in Figures 2 and 3 together we successfully demonstrated how NanoSPR provides a new and powerful tool for the parallel study of many macromolecular interactions. It is made possible by the combination of our fast and automated optical dark-field spectroscopy system with the flexible particle functionalization via His-tags. For this functionalization, it turned out to be important to first stabilize the gold nanorods with short DNA oligomers, which prevent aggregation in saline solutions.

Assuming the availability of a large library of His-tagged proteins and an automated sensor fabrication process, we see no fundamental or practical limitations to extend the parallelization over at least 2 orders of magnitude. Currently, we have a maximum of 1000 particles or sensing elements in the field of view, which would limit the number of different proteins to study to 20−50. Considering that the field of view represents only a very small fraction of the actual flow cell device we use, a larger scan area could easily extend the number of investigated particles. The limitations of NanoSPR, regarding the measurable range of K_D values, should be equivalent to those for conventional SPR. At the lower end, it is limited by the measurement accuracy and the time needed to reach equilibrium. In our current system, the detection limit was estimated to be around 1 nM,[24] providing a lower limit of measurable K_D values 1 order of magnitude higher, that is, with values of around 10 nM.[33] The upper limit (for low affinity interactions) is difficult to estimate and should be limited mostly by the solubility of the target molecule. In principle, a parallel study consisting of interaction pairs showing very different K_D values should be possible. An example with K_D = 0.7 μM and K_D = 25.2 μM is shown in the Supporting Information (Figure S5). If even larger differences in K_D are possible to observe, it remains to be tested, but we see no reason to doubt this. With regards to the limit to measure low molecular mass molecules, NanoSPR should have advantages over conventional SPR because the sensing volume is better matched to molecular dimensions.[34,35] Tuning the nanorod dimensions affects the sensing volume that can be used to optimize the NanoSPR sensors for either low or high molecular mass target molecules.[34] NanoSPR shares with all surface techniques (like SPR) the issue of possible influence of the immobilization of one binding partner on the binding strength with the target. In other words, the immobilization should not affect to the binding place and the target protein should have good accessibility, both of which need to be checked independently.

We see at least three more possible advantages of NanoSPR compared to conventional SPR: the nanoscopic dimension of the sensing elements drastically reduces the problem of nonuniform surface functionalization across the SPR sensor surface,[7] drastically reduces the required sample volume, and provides a build-in statistics without the need to repeat the

dx.doi.org/10.1021/nl501865p | Nano Lett. 2014, 14, 5528−5532

measurement. These advantages make NanoSPR a simple, fast, and cost-effective route to characterize binding affinities between many macromolecular partners simultaneously. We envision NanoSPR to be especially useful for the study of biochemical and biomedical processes in vitro and envision it to be useful for screening applications, for example, for lead generation in the drug discovery process.

■ ASSOCIATED CONTENT

Supporting Information

Detailed information on particle characterization and SPR measurements are provided. This material is available free of charge via the Internet at http://pubs.acs.org.

■ AUTHOR INFORMATION

Corresponding Authors

*E-mail: (C.S.) soennichsen@uni-mainz.de.
*E-mail: (G.R.) grivas@cib.csic.es.

Author Contributions

The manuscript was written through contributions of all authors. All authors have given approval to the final version of the manuscript.

Notes

The authors declare no competing financial interest.

■ ACKNOWLEDGMENTS

This work was financially supported by the ERC Grant 259640 ("SingleSense"). J.P. was financially supported by the graduate school of excellence Materials Science in Mainz. This work was supported by the Spanish government through Grant BIO2011-28941-C03-03 to G.R. We thank to Noelia Ropero and Víctor Hernández-Rocamora for protein production and useful comments.

■ REFERENCES

(1) Han, J.-D. J.; Bertin, N.; Hao, T.; Goldberg, D. S.; Berriz, G. F.; Zhang, L. V.; Dupuy, D.; Walhout, A. J. M.; Cusick, M. E.; Roth, F. P.; Vidal, M. *Nature* **2004**, *430*, 88−93.
(2) Howell, J. M.; Winstone, T. L.; Coorssen, J. R.; Turner, R. J. *Proteomics* **2006**, *6*, 2050−69.
(3) Pandey, A.; Mann, M. *Nature* **2000**, *405*, 837−846.
(4) Erickson, H. P.; Anderson, D. E.; Osawa, M. *Microbiol. Mol. Biol. Rev.* **2010**, *74*, 504−528.
(5) Mingorance, J.; Rivas, G.; Vélez, M.; Gómez-Puertas, P.; Vicente, M. *Trends Microbiol.* **2010**, *18*, 348−356.
(6) Vicente, M.; Rico, A. I. *Mol. Microbiol.* **2006**, *61*, 5−8.
(7) Schuck, P. *Annu. Rev. Biophys. Biomol. Struct.* **1997**, *26*, 541−566.
(8) Fee, C. *Methods Mol. Biol.* **2013**, *996*, 313−322.
(9) Bleicken, S.; Otsuki, M.; García-Sáez, A. J. *Curr. Protein Pept. Sci.* **2011**, *12* (8), 691−8.
(10) Velázquez-Campoy, A.; Leavitt, S. A.; Freire, E. *Methods Mol. Biol.* **2004**, *261*, 35−54.
(11) Howlett, G. J.; Minton, A. P.; Rivas, G. *Curr. Opin. Chem. Biol.* **2006**, *10*, 430−6.
(12) Knezevic, J.; Langer, A.; Hampel, P. A.; Kaiser, W.; Strasser, R.; Rant, U. *J. Am. Chem. Soc.* **2012**, *134*, 15225−8.
(13) Homola, J.; Vaisocherová, H.; Dostálek, J.; Piliarik, M. *Methods* **2005**, *37*, 26−36.
(14) Washburn, A. L.; Bailey, R. C. *Analyst* **2011**, *136*, 227−236.
(15) Anker, J. N.; Hall, W. P.; Lyandres, O.; Shah, N. C.; Zhao, J.; Van Duyne, R. P. *Nat. Mater.* **2008**, *7*, 442−53.
(16) McFarland, A. D.; Van Duyne, R. P. *Nano Lett.* **2003**, *3*, 1057−1062.
(17) Sönnichsen, C.; Franzl, T.; Wilk, T.; von Plessen, G.; Feldmann, J.; Wilson, O.; Mulvaney, P. *Phys. Rev. Lett.* **2002**, *88*, 077402-(1−4).
(18) Ahijado-Guzmán, R.; Gómez-Puertas, P.; Alvarez-Puebla, R. A.; Rivas, G.; Liz-Marzán, L. M. *ACS Nano* **2012**, *6*, 7514−20.
(19) Wang, Y.; Tang, L.-J.; Jiang, J.-H. *Anal. Chem.* **2013**, *85*, 9213−9220.
(20) Wang, J.; Dong, B.; Chen, B.; Jiang, Z.; Song, H. *Dalton Trans.* **2012**, *41*, 11134−11144.
(21) Singh, A. K.; Senapati, D.; Wang, S.; Griffin, J.; Neely, A.; Candice, P.; Naylor, K. M.; Varisli, B.; Kalluri, J. R.; Ray, P. C. *ACS Nano* **2009**, *3*, 1906−1912.
(22) Yu, C.; Nakshatri, H.; Irudayaraj, J. *Nano Lett.* **2007**, *7*, 2300−2306.
(23) Joshi, P. P.; Yoon, S. J.; Hardin, W. G.; Emelianov, S.; Sokolov, K. V. *Bioconjugate Chem.* **2013**, *24*, 878−888.
(24) Rosman, C.; Prasad, J.; Neiser, A.; Henkel, A.; Edgar, J.; Sönnichsen, C. *Nano Lett.* **2013**, *13*, 3243−3247.
(25) Ohashi, T.; Hale, C. A.; de Boer, P. A.; Erickson, H. P. *J. Bacteriol.* **2002**, *184*, 4313−5.
(26) Rico, A. I.; Krupka, M.; Vicente, M. *J. Biol. Chem.* **2013**, *288*, 20830−6.
(27) Dajkovic, A.; Lan, G.; Sun, S. X.; Wirtz, D.; Lutkenhaus, J. *Curr. Biol.* **2008**, *18*, 235−44.
(28) Hu, Z.; Mukherjee, A.; Pichoff, S.; Lutkenhaus, J. *Proc. Natl. Acad. Sci. U.S.A.* **1999**, *96*, 14819−24.
(29) Schuck, P.; Millar, D. B.; Kortt, A. A. *Anal. Biochem.* **1998**, *265*, 79−91.
(30) Hernández-Rocamora, V. M.; García-Montanés, C.; Reija, B.; Monterroso, B.; Margolin, W.; Alfonso, C.; Zorrilla, S.; Rivas, G. *J. Biol. Chem.* **2013**, *288*, 24625−35.
(31) Hernández-Rocamora, V. M.; Reija, B.; García, C.; Natale, P.; Alfonso, C.; Minton, A. P.; Zorrilla, S.; Rivas, G.; Vicente, M. *J. Biol. Chem.* **2012**, *287*, 30097−104.
(32) Martos, A.; Alfonso, C.; López-Navajas, P.; Ahijado-Guzmán, R.; Mingorance, J.; Minton, A. P.; Rivas, G. *Biochemistry* **2010**, *49*, 10780−7.
(33) Tellinghuisen, J. *Anal. Biochem.* **2012**, *424*, 211−220.
(34) Ament, I.; Prasad, J.; Henkel, A.; Schmachtel, S.; Sonnichsen, C. *Nano Lett.* **2012**, *12*, 1092−5.
(35) Otte, M. A.; Sepúlveda, B.; Ni, W.; Juste, J. P.; Liz-Marzán, L. M.; Lechuga, L. M. *ACS Nano* **2009**, *4*, 349−357.